Science Press

ARTICLE

Effect of Mechanical Characteristics of Gold Wire on Microstructure and Properties of Ball Bonding

Kang Feifei[1], Zhou Wenyan[1], Yu Jianshu[1], Ji Xingqiao[2], Wang Jia[1], Chen Xubo[2], Luo Jianqiang[2], Liang Chen[1], Wu Yongjin[1], Pei Hongying[1]

[1] *State Key Laboratory of Advanced Technologies for Comprehensive Utilization of Platinum Metals, Sino-platinum Metals Co., Ltd, Kunming 650106, China;* [2] *The 29th Research Institute of CETC, Chengdu 610036, China*

Abstract: Microstructure of gold wires with different mechanical characteristics was characterized by electron backscattering diffractometer. The loop profile, the heat affected zone and bonding point morphology were observed by scanning electron microscopy and optical microscopy, and the pulling force and ball shear force were measured by push-pull tester. Finally, the influence of mechanical characteristics of gold wires on the ball bonding quality was analyzed. The results show that there is obvious difference in microstructure along the radial direction. The core of the gold wire in semi-hard state 1 and 2 retains fibrous structure, and the edge grains are fine equiaxed grains. The length of the heat affected zone (HAZ) formed after forming the ball is short, the structure of the ball neck has obvious step, and the loop height after bonding is small compared with the soft state. The soft gold wire shows coarser equiaxed crystal, lower pulling force, and is prone to ball slip. The gold wire in semi-hard 2 state has strong bonding force to the pad, high pulling force and excellent overall bonding quality, which is the most suitable for the ball bonding process.

Key words: gold wire; ball bonding process; mechanical characteristics; heat affected zone length; bonding quality

Gold wire is a bonding material with stable chemical performance, good ductility and strong weldability. As a key basic material for MEMS, MiniLED, microwave RF devices and 5G communication, it is used for the connection between chip and chip, chip and substrate[1-3]. In order to develop a fine and customized service system for different fields of application, it is necessary to study the adaptability of gold wire to different bonding processes. Ball bonding and wedge bonding are two common wire bonding methods. Ball bonding has no directivity and its bond strength is generally greater than that of wedge bonding in similar electrode systems[4]. The process of ball bonding involves the formation of air-free welding ball by the tip of the gold wire through the discharge of an electric spark, and the wire is bonded to the chip by the ultrasonic vibration of the capillary, the pressure, and the high temperature of the bonding surface (typically 150 °C)[5].

The ball bonding process is a complex deformation process, which is always accompanied by the change of microstructure and stress[6]. In the wire bonding process of multi-layer and multi-row pad shell packaging circuit, it is necessary to control not only the quality of the bonding point, but also the loop profile and mechanical strength of each layer of the bonding wire to meet the requirements for process control. The higher the hardness of the bonding wire, the stronger the anti-vibration ability, and the lower the probability of wire collapse during the encapsulation and thermal shock process. Thus, the bond quality problems due to short circuit caused by wire collapse can be reduced. Therefore, the high hardness of bonding wires is beneficial for controlling the loop[7], but the excessive hardness will cause the craters, which reduces the reliability of the device on the contrary. While the electronic device is working, the gold wire is continuously subjected to mechanical stress and strain. The main causes of these stress

and strain formations include temperature cyclic loads due to the different thermal expansion coefficients between electronic components and circuit boards, and mechanical cyclic loads due to frequent sloshing under certain circumstances. In order to ensure the reliability of electronic equipment, the bonding wire must have certain mechanical properties to resist the impact force from other component or materials[8]. Therefore, the mechanical characteristics of the gold wire have an important influence on the loop control and the formation of solid solder joints after bonding, especially in the complex packaging forms with multilayer, high density and multiple bonding modes, or components with high reliability requirements[9]. Some research results have been reported on the relationship between mechanical properties of gold wire and the bonding quality. For example, the texture of the gold wire formed during drawing is adjusted by isothermal annealing to form the final grain orientation. In the process of gold ball formation, the grain orientation at the center of the ball is consistent with the core of the base wire, and the grain orientation is closely related to the properties of the wire, indicating that the grain orientation of the base wire will affect the bonding properties[10,11]. For another example, the recrystallization temperature of gold wire is one of the factors affecting the length of heat affected zone[12,13]. The inhomogeneity of gold wire texture will cause loop drooping, and the main failure mode is wire bending fatigue failure[14]. However, for the ball bonding process, it is still unclear to what level the mechanical characteristics of gold wire should be controlled to achieve the best bonding quality.

On this basis, three types of gold wires with different mechanical characteristics were designed and the microstructure before and after ball bonding process and bonding properties were characterized. The state of the gold wire suitable for the gold ball bonding process was studied, and the relationship between the performance of the base wire, the microstructure and the application performance was established, which provides technical guidance for the precise application of gold wire, as well as basic data for the design and development of next-generation bonding wire materials.

1 Experiment

The gold wire used in the experiment is made of gold with a purity ⩾99.999% and 10~100 μg/g cerium. The wire with a diameter of 25 μm was fabricated through the forward repeated drawing process after continuous casting of a Φ8 mm rod. Continuous annealing was carried out at 25, 200, 400, 450, 465 and 500 °C, with a speed of 45 m/min. The breaking load and elongation of the gold wire were measured by the single fiber strength tester (YM-06A) at 20 mm/min. According to the test results, the annealing curve was drawn, and three different states of gold wire were selected as the research object, which were labeled as sample I, II and III.

The three gold wire samples were bonded to the 2835 LED lights by high-speed wire bonding machine (HANs-5200 series). The free air ball was formed with a current of 14~23 mA and a discharge time of 6~14 s. The bonding power was 12%~18%, and the pressure was 25~40 g for the first bonding point, while the bonding power was 25%~30% and the pressure was 160~180 g for the second bonding point. After a free air ball was formed by spark discharge, a sample of 5 cm (the distance to the top of the ball) was intercepted with scissors, and then the longitudinal section of the sample was obtained by focused ion beam (FEI versa 3D) with length of 100~500 μm. The microstructure of the wire and the gold ball and neck was characterized by electron backscatter diffractometer (METEK 9424.079.60330STBC). The pulling force of the bonded wire and the shear force of the bonded ball were tested by the multifunctional push-pull tester (4000 type). Double beam electron microscope (FEI Versa 3D) and stereo microscope (STEMI2000-C) were used to observe the morphology of the loop; the first and the second bonding point, and the length and width of the fish tail were measured.

2 Results and Discussion

2.1 Mechanical property

Fig. 1 shows the variation of breaking load and elongation of the gold wire with annealing temperature. With the increase of temperature, the breaking load decreases sharply from 0.235 N to 0.078 N at room temperature. The elongation first remains stable and then rises sharply from 2% to 18%. When the temperature is 400~450 °C, the elongation of gold wire gradually increases, and the gold wire begins to recrystallize. At 465 °C, the elongation reaches about 5%. The elongation increases sharply at 465~500 °C, reaching 18%. Three typical states (elongation of 2.45%, 5.00% and 18.45%) as marked by the circles in Fig.1 are selected and labeled as sample I, II and III, respectively.

Fig. 2 shows the tensile stress-strain curves of the three samples. It can be seen that the gold wire has good plasticity and undergoes elastic deformation, plastic deformation and fracture during the tensile process. The plastic deformation stage of sample I is very short, and the fracture mechanism can be determined as brittle fracture. While, the ductility of sample III is good, and the fracture mechanism is ductile fracture. According to the rule that the area under the tensile stress-strain curve is approximately equal to the machining
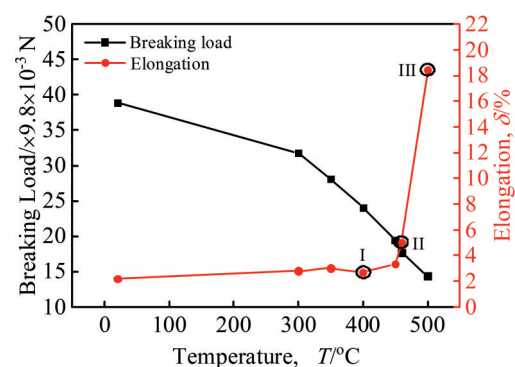

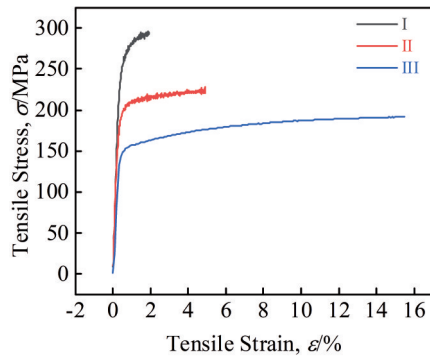Fig.1 Variation of tensile force and elongation with annealing temperature

Fig.2　Tensile stress-strain curves of three gold wire samples

toughness, the machining toughness of sample III is the best, and that of sample I is the worst. Based on the above analysis, it is considered that sample I and II are in the semi-hard state, marked as semi-hard state 1 and semi-hard state 2, respectively, and sample III is in the soft state.

2.2 Microstructure of wire and first bonding ball

Fig. 3 shows the crystallographic morphologies of three samples from the longitudinal section. Fig. 4 shows the distribution of grain orientation angle of the three samples. It can be seen from Fig. 3 that sample I has a fibrous structure with a grain size of 0.17~0.52 μm in the core. The edge of the wire begins to recrystallize which is composed of equiaxed crystal with the grain size in the range of 0.1~2.6 μm, and the average grain size is 0.26 μm. This indicates that the recrystallization time of the edge is earlier than that of the core, and there is inhomogeneity in the microstructure. In the histogram of grain orientation deviation angle distribution of sample I, there are two obvious peaks. One is between 0°~10°, indicating that these grains have the same or similar grain orientation, and the high proportion of small angle grain boundaries indicates that the effect of dislocation strengthening is significant. The other peak is between 50°~60°. These grains have large orientation deviation angles, which correspond to high energy grain boundaries and can effectively hinder the propagation of brittle fracture cracks[15,16]. The crystal morphology of sample II is similar to that of sample I, both consisting of fibrous and equiaxed grains. However, the grain size of sample II is significantly larger than that of sample I, with the grain size in the range of 0.2~4.8 μm and a large size deviation. Some grains grow abnormally, and some grains still maintain the initial state of recrystallization. The histogram trend of grain orientation deviation angle distribution of sample II is similar to that of sample I with two peaks, but the proportion of grain boundary with large angle is significantly higher than that of small angle, indicating that it has a stronger ability to prevent brittle fracture. All grains of sample III appear as equiaxed grains. The grain size ranges from 0.1 μm to 3.0 μm with the average grain size of 0.45 μm. But there is only one peak in the angle distribution of grain orientation deviation, namely the large angle grain boundary, which indicates that there is no dislocation strengthening in the gold wire.

In the process of ball bonding, tail of the three samples is ignited by electric spark to form a round gold ball[17]. Fig. 5 shows the longitudinal cross sections of the gold ball, the ball neck and the base wire. Grains of the gold ball grow along the direction of the wire and appear as coarse columnar crystals.
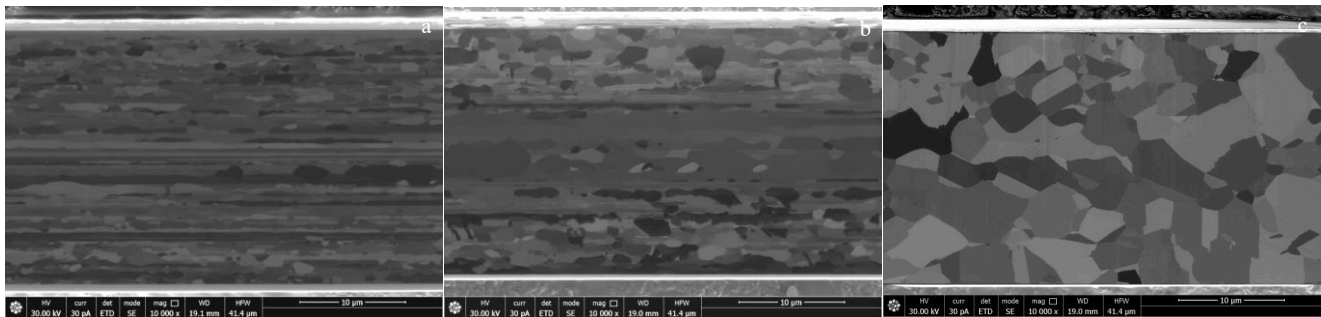

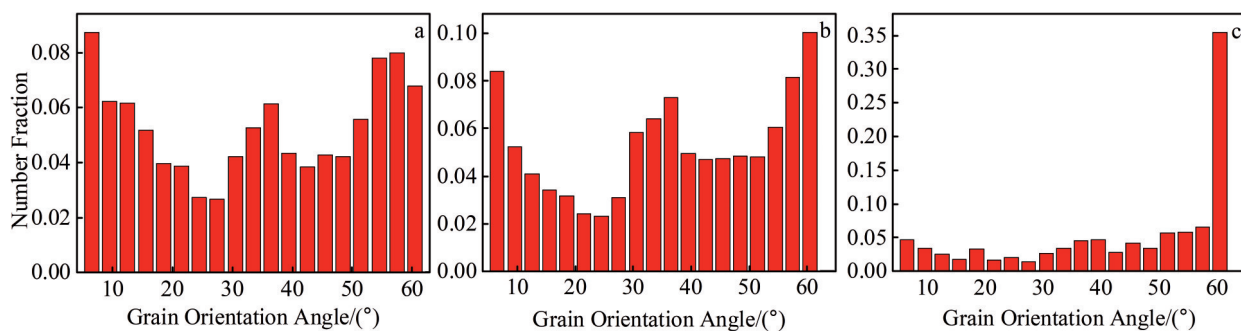Fig.3　Crystal morphologies of three samples: (a) I, (b) II, and (c) III

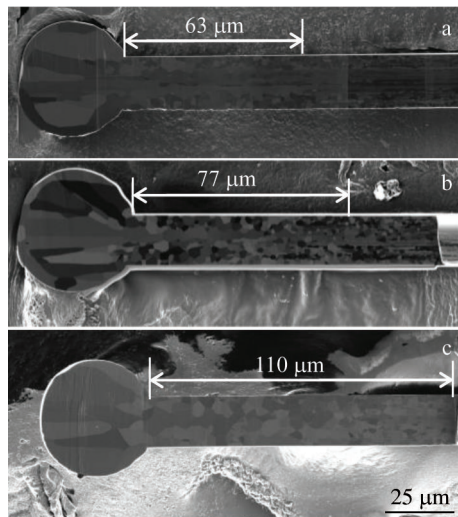Fig.4　Distribution of grain orientation angle of three samples: (a) I, (b) II, and (c) III

Fig.5   Longitudinal section microstructures of gold ball, ball neck and base wire of three samples: (a) I, (b) II, and (c) III

Fig.6   Top view of the lamp cup (a) and the front view (b) of the wire loop after bonding of sample I

Equiaxed grains are formed in the neck of the ball under the influence of heat. The further away from the gold ball, the less the influence of electric spark and the smaller the grain size. The morphology of the ball neck has obvious step characteristic. Compared with the base wire, the grains in the ball neck region of sample I grow significantly, but the fibrous structure in the core still remains. The grains at the edge of the wire in the ball neck region of sample II also grow significantly, and the grains at the core change from the fiber of the base wire to equiaxed grain, indicating that the recrystallization of the core material has occurred during the ball forming process. The grain size of sample III is almost twice larger than that of the base wire. By measuring the heat affected zone (HAZ) length of the three gold wires, sample I has the shortest HAZ length (63 μm), followed by sample II (77 μm), and sample III (110 μm). The microstructure and length of the HAZ are also different because of different mechanical characteristics and microstructure of the base wire. The loop height of the gold wire after bonding is directly determined by the HAZ length. The longer the HAZ length, the higher the loop height[18].

2.3 Bonding property

Fig.6 shows the top view of the lamp cup and the front view of the wire loop after bonding of sample I. The wire loop is stable without skew or collapse. The distance between the chip and the highest point of the wire loop is called the loop height H. The wire loop is divided into two sections: heat affected zone and base wire zone[19,20]. Under the action of ultrasonic, heat and pressure, the gold ball is pressed on the pad to form the first bonding point, and the ball is metallurgically bonded with the metallization layer on the pad surface. The second bonding point is made by the pressure and ultrasonic of the capillary to combine the gold wire and the frame, and the morphology is like a fish tail. The morphologies of the first and second bonding point of the three samples are shown in Fig. 7. The size of fish tails was
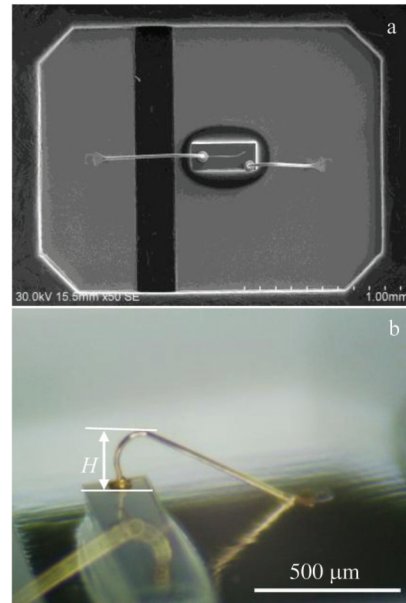
measured, and the relationship between mechanical characteristics of the gold wire and bonding quality was studied. Under the bonding pressure, the gold ball becomes a round cake, the surface is honeycomb, and there is a step in the area where the wire meets the ball. The first bonding point surface of sample I has a small angle with the wire, and micro cracks are found at the joint (shown by arrow). There is no capillary mark on the fish tail but a gap between the fish tail and the bonding joint on the surface of the frame, indicating that the bonding force is not strong. The first bonding point of sample II are relatively round, and the fish tail has an obvious capillary mark. The connection line with the bonding points on the surface of the frame is longer, and the gap is shorter. The first bonding point of sample III has the phenomenon of sliding ball with a protruding bonding edge. The loop on the top of the bonding ball shows a torsion, and the fish tail has a slight capillary mark. The connecting wire with the bonding point on the surface of the frame is short, and the gap is obvious. Table 1 shows the loop characteristic parameters and bonding properties. As can be seen, the loop heights of the three samples show a relationship of I<II<III, which is in consistent with the trend of the heat affected zone length. The fish tail length and width of sample II are obviously larger than those of sample I and sample III, indicating that its second bonding point has the largest deformation. Stress concentration occurs in the loop torsion of sample III. It has a thicker fish tail and both of the wire pulling force and ball shear force are smaller than those of sample II. The reason is that under the same bonding pressure, deformation at the first bonding point of sample III is the largest because it is the softest among the three wires. It is prone to the gold ball overflow, which reduces the bonding strength to the electrode. Wire pulling force and ball shear force of the three samples
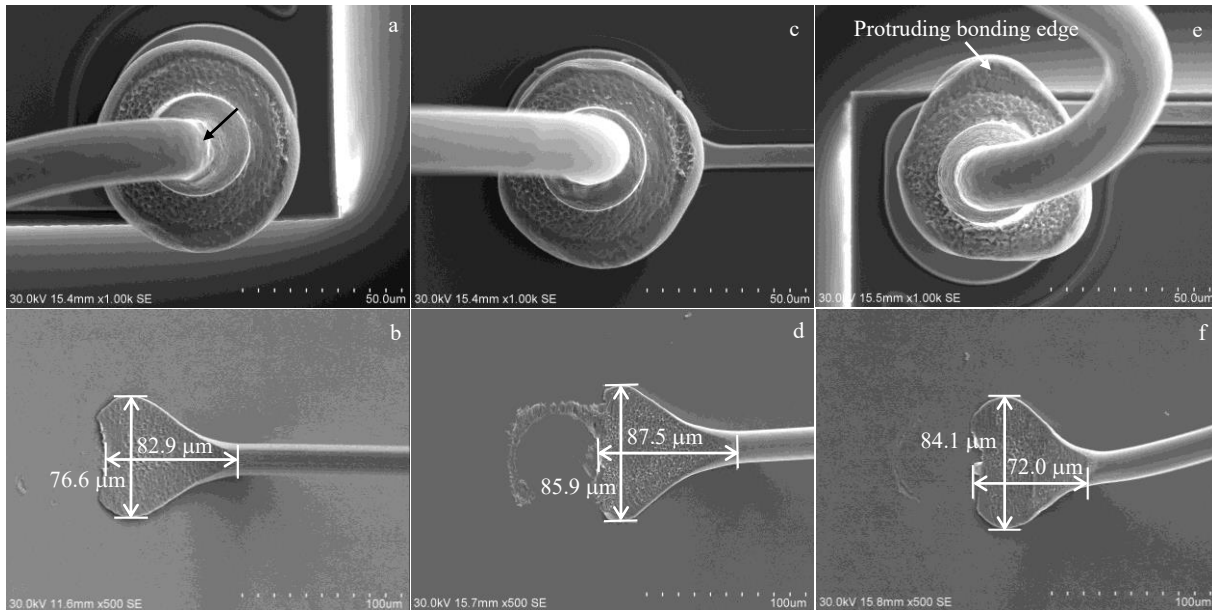
Fig.7   Morphologies of the first bonding ball (a, c, e) and the second bonding tail (b, d, f) of the three samples: (a, b) I, (c, d) II, and (e, f) III

Table 1   Loop characteristics and bonding properties

Sample	Loop height, H/μm	Fish tail length, L/μm	Fish tail width, D/μm	Wire pulling force, σ/×9.8×10^{-3} N	Failure type	Ball shear force/ ×9.8×10^{-3} N	Tail shear force/ ×9.8×10^{-3} N
I	231.28	82.9	76.6	9.0~10.0	Ball neck broken	44~56	62~78
II	250.83	87.5	85.9	9.6~10.5	Ball neck broken	46~55	63~81
III	283.75	72.0	84.1	8.4~9.5	Ball neck broken	35~50	58~66

shows a relationship as III<I<II.

Combined with the microstructure analysis, the bonding properties of gold wires in different states are discussed. Sample I is in state of semi-hard 1, and the base wire and the ball neck are composed of equiaxed grains at the edge and fibrous grains at the core. In the continuous annealing process, the core of the gold wire still retains the fibrous structure, while the edge is recrystallized, forming small equiaxed grains with many grain boundaries. Gold wire shows high strength under the synergistic effect of work hardening and fine grain strengthening. In the process of thermo-ultrasonic bonding, the ball neck is instantly deformed, which will lead to serious stress concentration. If the gold wire itself has high strength, its plastic deformation ability is insufficient. Then the ball neck will produce more stress concentration. In the thermal shock test, the stress concentration will become a weak point, at which microcracks are prone to occur and continue to expand until fracture [21]. In addition, due to the higher hardness of semi-hard 1 gold wire, higher power and pressure are often required to obtain good bonding strength during bonding. However, the increase of bonding parameters will produce craters, cracks and other defects, which bring risk to the reliability of components. Compared with semi-hard 1, sample II in semi-hard 2 shows less fibrous grains in the core and larger equiaxed grains at the edge. During electronic fire off (EFO), the fibrous structures at the core are recrystallized,

which makes the perfect combination of plastic and toughness at the ball neck, so the highest bonding strength can be obtained. Bonding joint deformation of soft state gold (sample III) is large, which is prone to ball sliding. In high-density packaging chip, it can cause short circuit or open circuit problem. What's more, the length of the heat affected zone is larger and the loop is higher. In the process of encapsulation, the loop is easy to skew under the impact force, resulting in short circuit due to the collision of adjacent loop. Therefore, the gold wire in semi-hard 2 is the most suitable for ball bonding.

3 Conclusions

1) The initial recrystallization temperature of gold wire is 400 °C, at which it is in a semi-hard state with an elongation of 2.45%. When the annealing temperature is 450 °C, the wire is still semi-hard and the elongation is 5.00%. As the annealing temperature reaches 500 °C, the gold wire is in soft state and the elongation is 18.45%.

2) The core of gold wires in semi-hard 1 and semi-hard 2 retains fibrous structure while the edge becomes equiaxed crystals. The recrystallization of gold wire starts from the edge, and the regional imbalance results in the coexistence of two kinds of microstructure. The gold wire in soft state is equiaxed in the whole radial direction and the grain size is obviously larger than that of the semi-hard state. The length of

heat affected zone (HAZ) of semi-hard gold wire is smaller than that of soft gold wire. The higher the ductility of base wire, the longer the HAZ length.

3) The fish tail of the gold wire in semi-hard 2 presents large deformation, good bonding with pad, high wire pulling force and ball shear force, and high comprehensive bonding quality, so it is the most suitable for ball bonding.

References

1 Gan Chong Leong, Hashim U. *Journal of Materials Science: Materials in Electronics*[J], 2015, 26: 4412

2 Gan C L, Classe F, Hashim U. *Materials Science: Microelectronics International*[J], 2014, 31(2): 121

3 Breach C D. *Gold Bulletin*[J], 2010, 43: 150

4 Alim Md Abdul, Abdullah M Z, Abdul Aziz M S *et al. Sensors and Actuators A: Physical*[J], 2021, 329: 112 817

5 Roslan Hafiz, Abdul Aziz M S, Abdullah M Z *et al. IOP Conference Series: Materials Science and Engineering*[J], 2020, 1007(1): 12 173

6 Li Chunmei, Yang Ping, Liu Deming *et al. Chinese Journal of Stereology and Image Analysis*[J], 2005, 10(4): 247

7 Yang Bing, Guo Daqi. *Electronics & Packaging*[J], 2007, 7(8): 1

8 Yao Lihua. *Electronics & Packaging*[J], 2010, 10(10): 31

9 Chang Qian, Zhu Yuan, Cao Yuyuan. *Electronics & Packaging*[J], 2017, 17(2): 4

10 Son Seoung Bum, Roh Hyunchul, Kang Suk Hoon *et al. Gold Bulletin*[J], 2011, 44: 231

11 Wulff, Breach C D, Dittmer K. *Journal of Materials Science Letters*[J], 2003, 22: 1373

12 Sun Lining, Liu Yuetao, Liu Yanjie. *Transactions of Nonferrous Metals Society of China*[J], 2009, 19(2): 490

13 Kim K S, Song J Y, Chung E K *et al. Mechanics of Materials*[J], 2006, 38: 119

14 Kung Huang Kuang, Chen Hung Shyong, Lu Ming Cheng. *Microelectronics Reliability*[J], 2013, 53: 288

15 Yin Shehui, Wang Jichang, Xu Pengfei. *Journal of Gansu Sciences*[J], 2014, 26(2): 30 (in Chinese)

16 Li Zhenliang, Tian Dongkuo. *Rare Metal Materials and Engineering*[J], 2021, 50(2): 639

17 Cao Jun, Fan Junling, Gao Wenbin. *Rare Metal Materials and Engineering*[J], 2018, 47(6): 1836 (in Chinese)

18 Shah Mithilesh, Zeng Kaiyang, Tay Andrew A O. *Journal of Electronic Packaging*[J], 2004, 126(1): 87

19 Li Junhui, Zhang Xiaolong, Liu Linggang *et al. Journal of Microelectromechanical Systems*[J], 2013, 22(3): 560

20 Tsai Chih Hsin, Chuang Chien Hsun, Tsai Hsing Hua *et al. IEEE Transactions on Components, Packaging and Manufacturing Technology*[J], 2016, 6(2): 298

21 Cao Jun. *Thesis for Doctorate*[D]. Lanzhou: Lanzhou University of Science, 2012: 144 (in Chinese)

金丝的力学特征对球键合的微观组织和性能的影响

康菲菲[1]，周文艳[1]，俞建树[1]，季兴桥[2]，王　佳[1]，陈绪波[2]，罗建强[2]，梁　辰[1]，吴永瑾[1]，裴洪营[1]

(1. 贵研铂业股份有限公司 稀贵金属综合利用新技术国家重点实验室，云南 昆明 650106)

(2. 中国电子科技集团第二十九研究所，四川 成都 610036)

摘　要：用电子背散射衍射仪对具有不同力学特征金丝的微区组织进行表征，采用扫描电镜和光学显微镜观察线弧轮廓、热影响区和焊点形貌，并通过推拉力测试仪测量线弧拉力和焊球剪切力，分析金丝力学特征对球键合质量的影响。结果表明：半硬态1和半硬态2的金丝芯部保持纤维状组织，边缘晶粒为细小的等轴晶，沿径向微区组织形貌有明显差异。打火烧球后形成的热影响区长度短，球颈部的组织有明显的梯度性，键合后弧高较小。软态金丝的组织为粗大的等轴晶，沿径向分布均匀，键合拉力低，易发生滑球现象。半硬态2金丝与焊盘的结合力强，引线键合拉力高，综合键合质量优，是最适合球键合工艺的金丝。

关键词：金丝；球键合工艺；力学特征；热影响区长度；键合质量

作者简介：康菲菲，女，1985年生，硕士，高级工程师，贵研铂业股份有限公司稀贵金属综合利用新技术国家重点实验室，云南 昆明 650106，电话：0871-68318299，E-mail：kff@ipm.com.cn